

# Figure S1

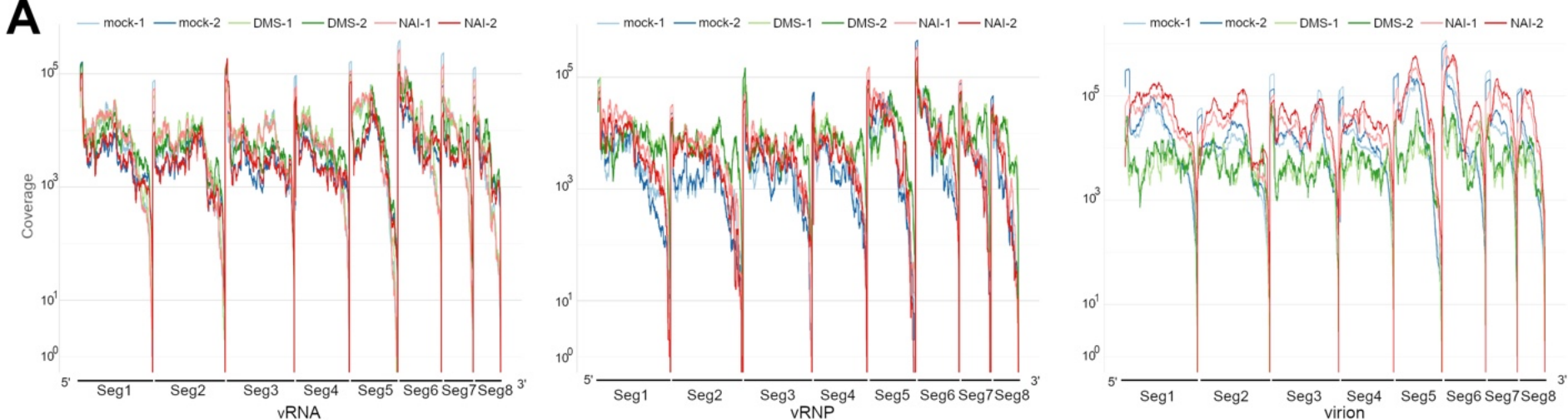
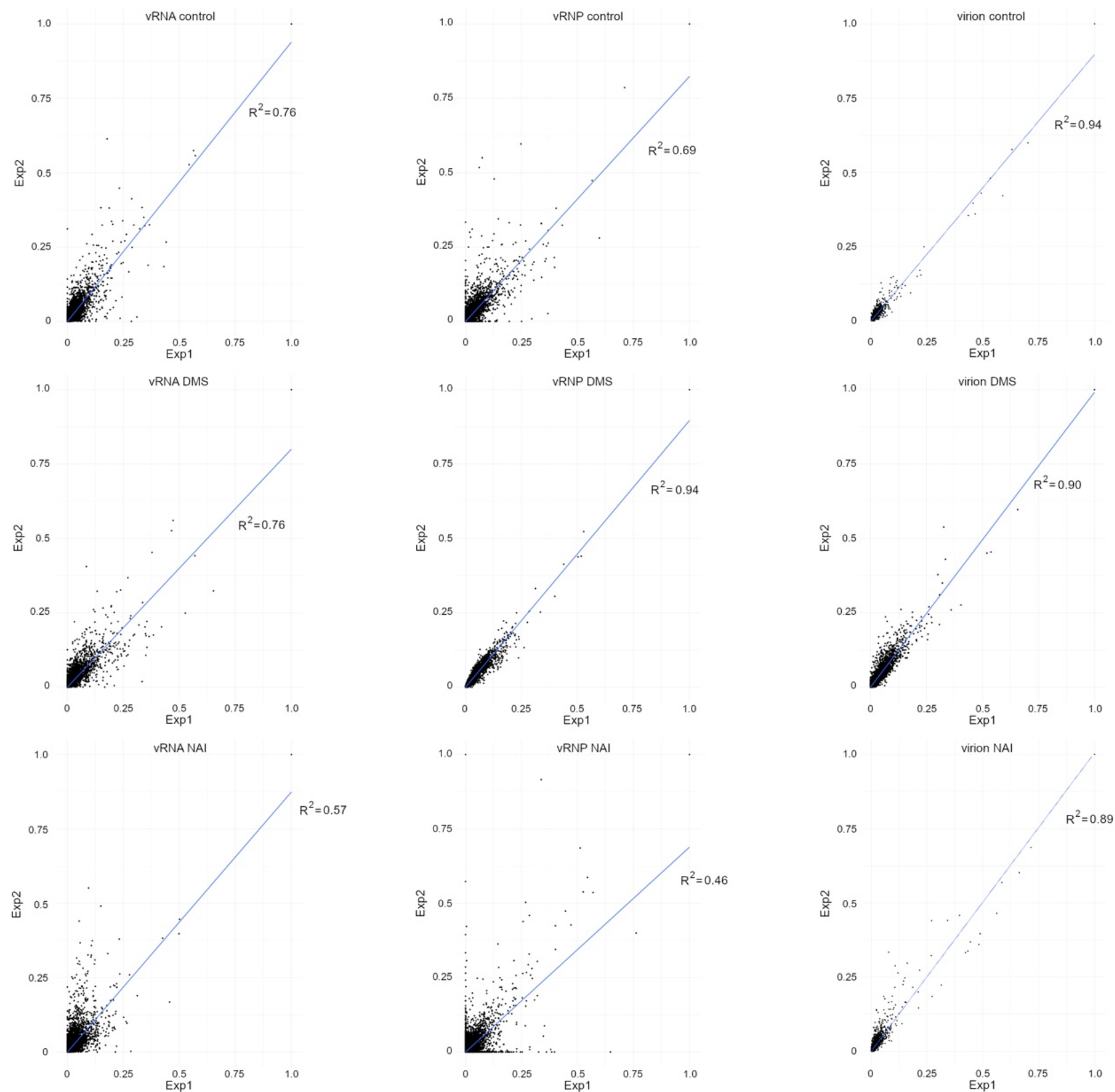
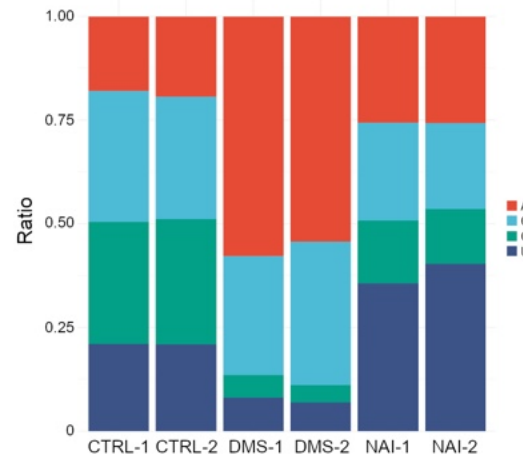
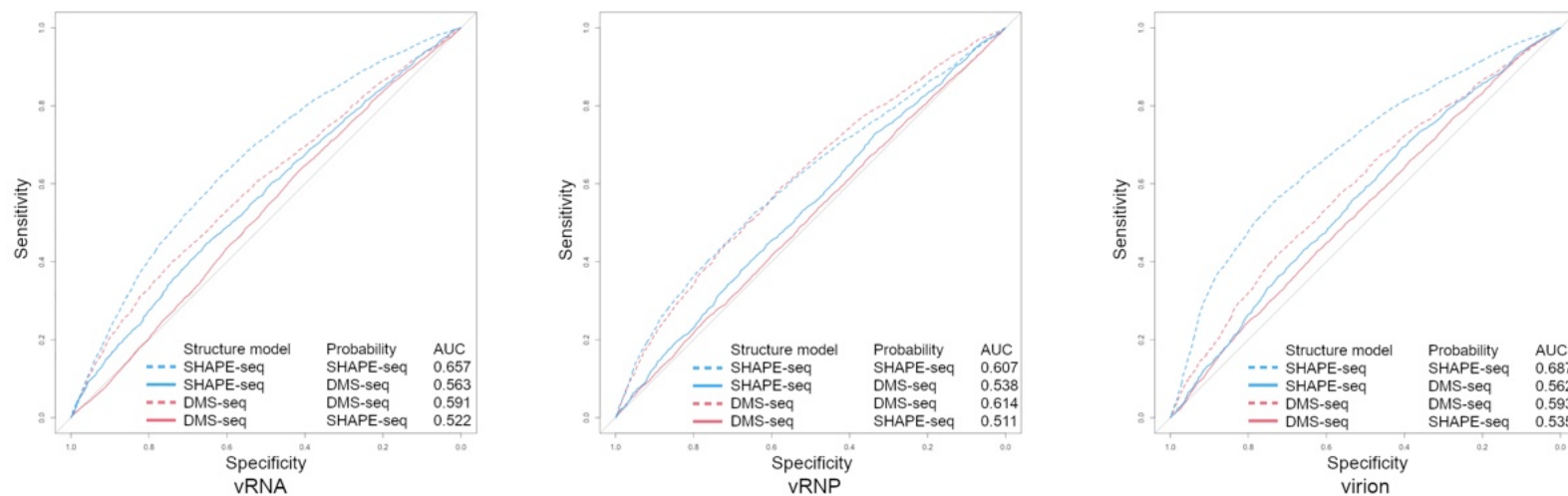
**A****B**

Figure S2

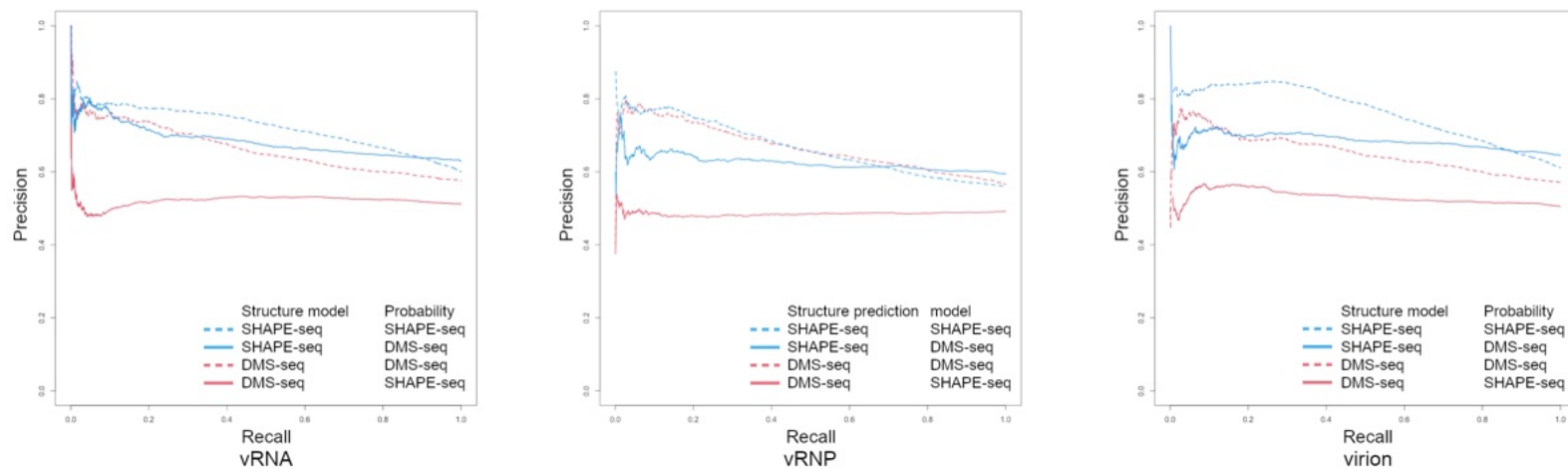
**A**



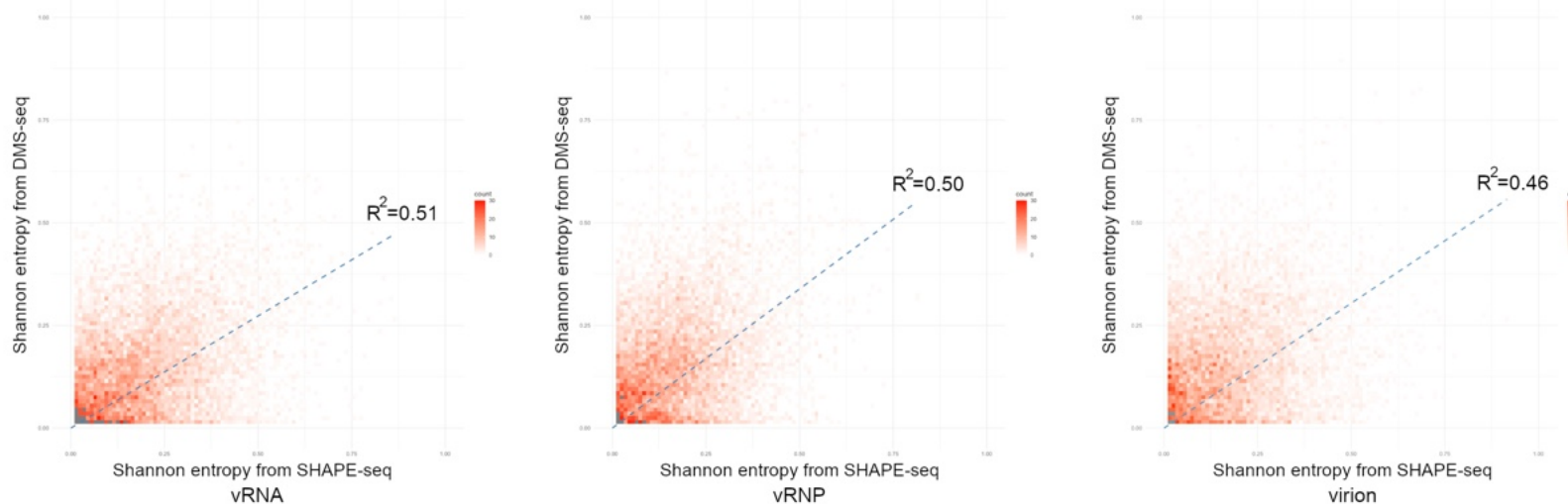
**B**



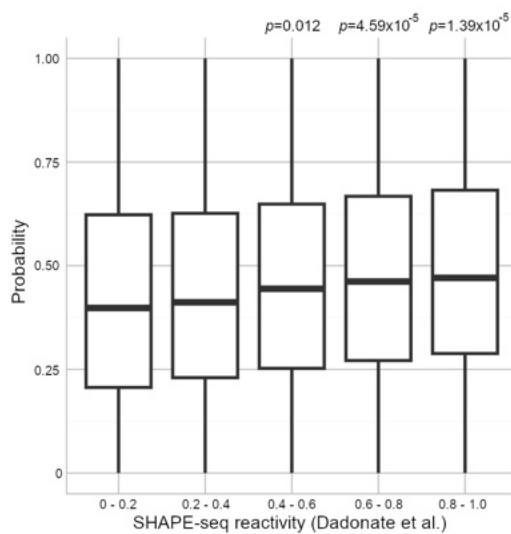
**C**



**D**



**E**



**F**

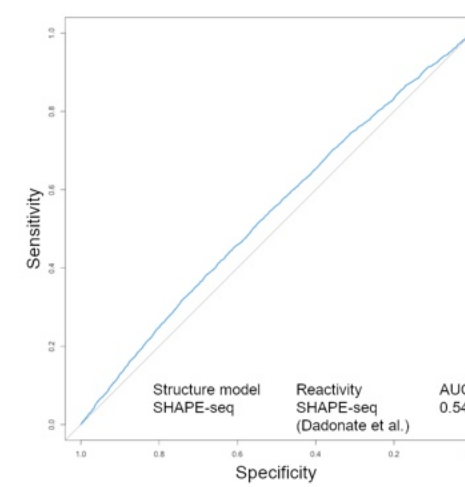
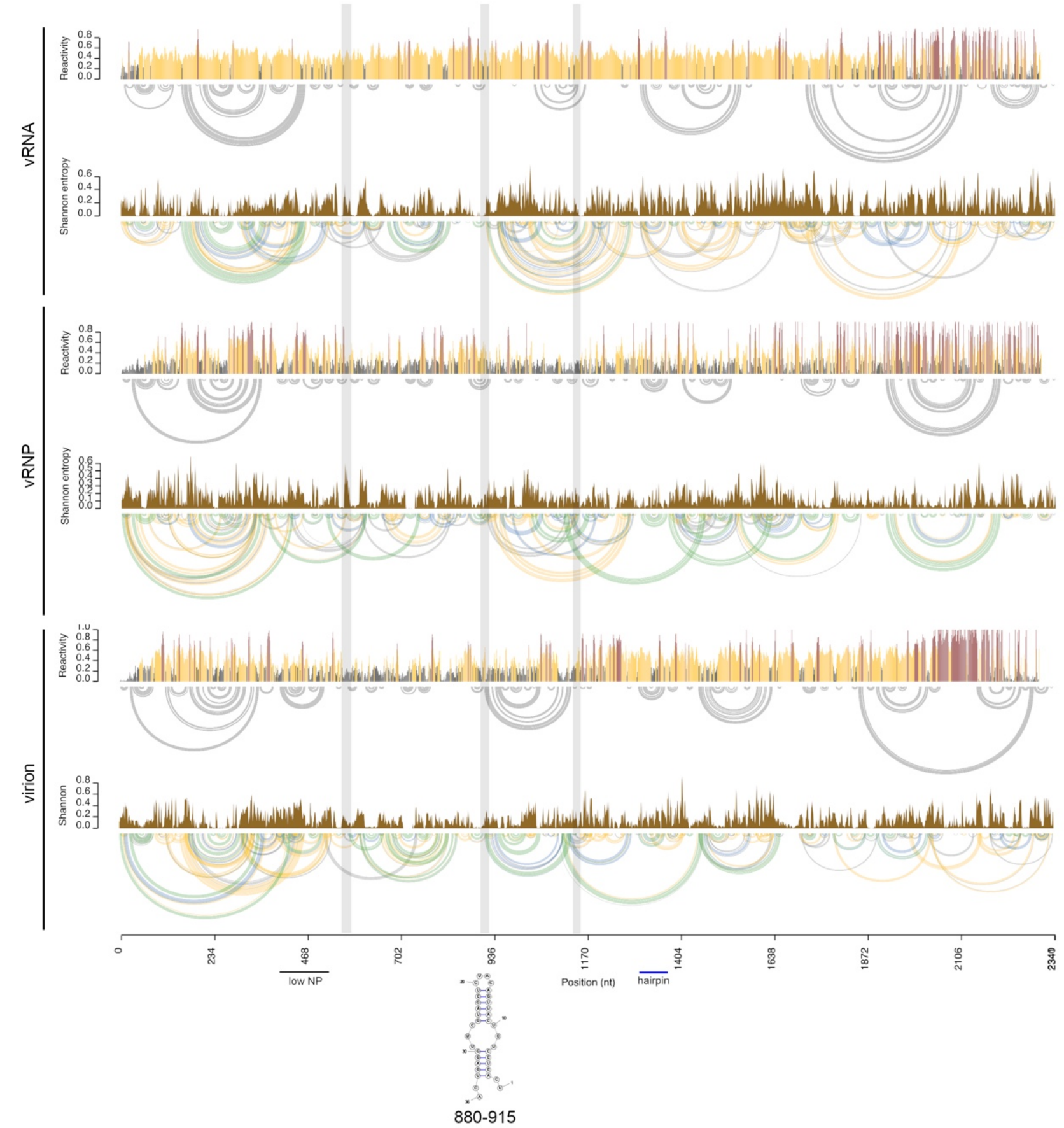
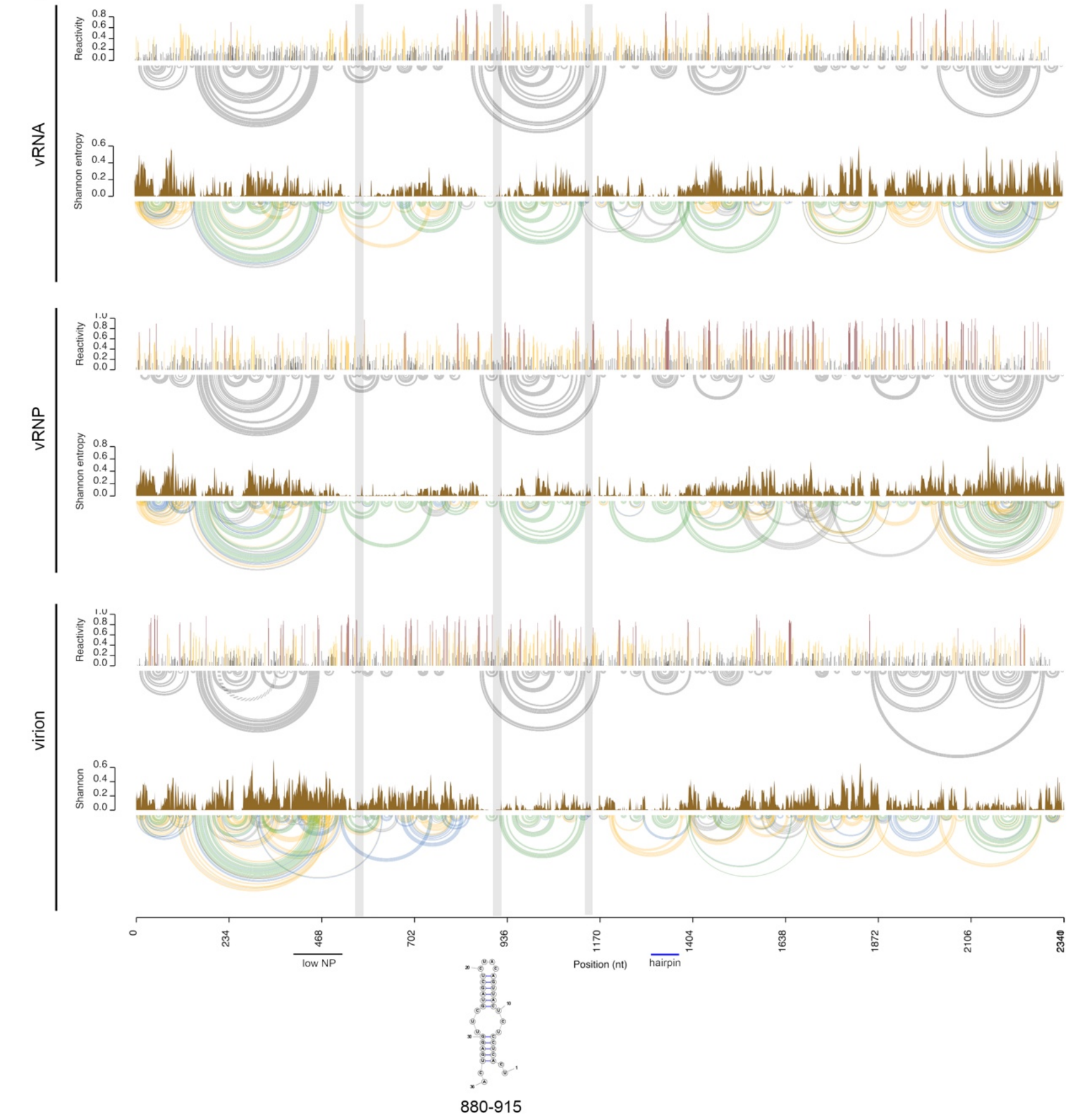
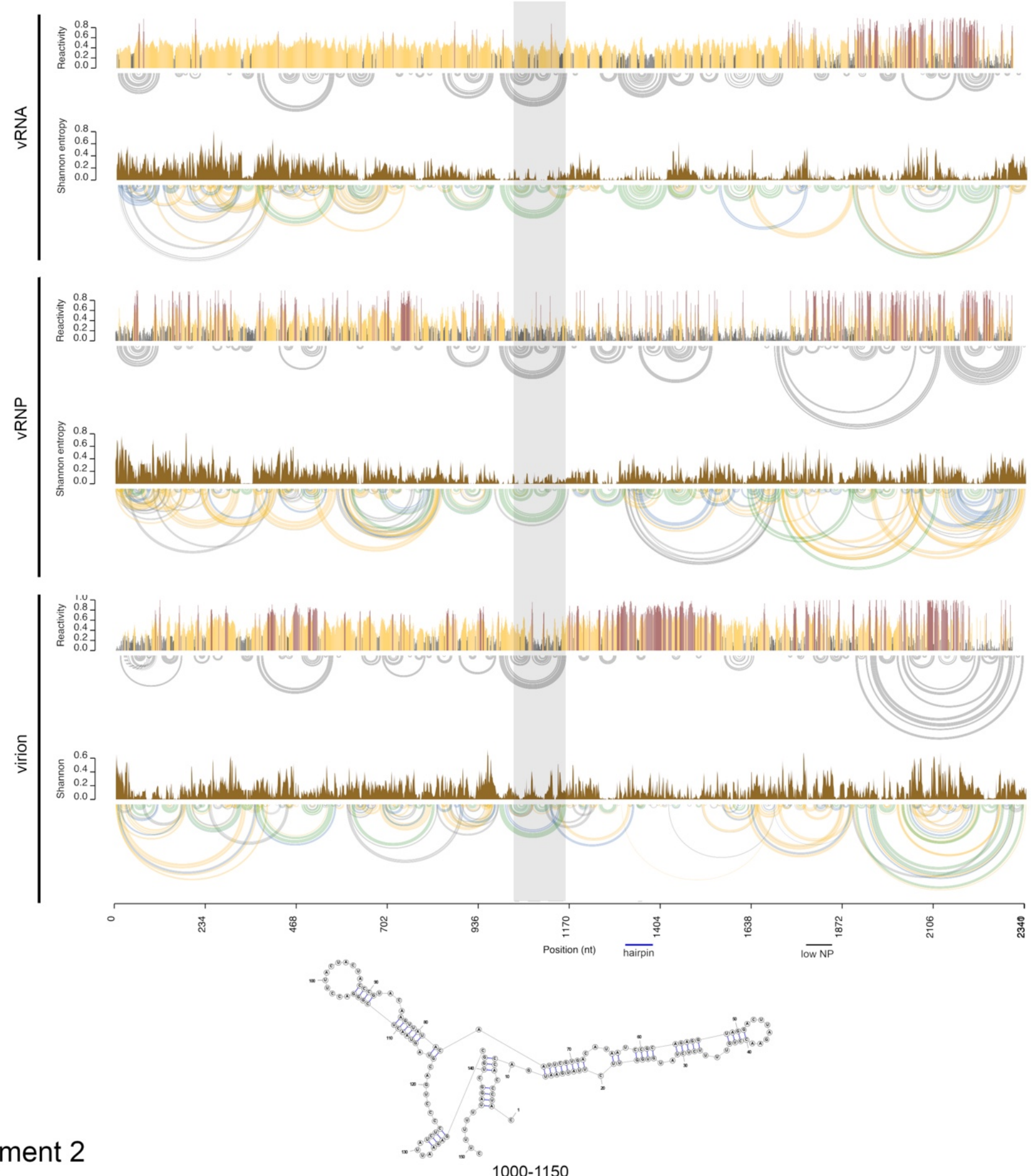
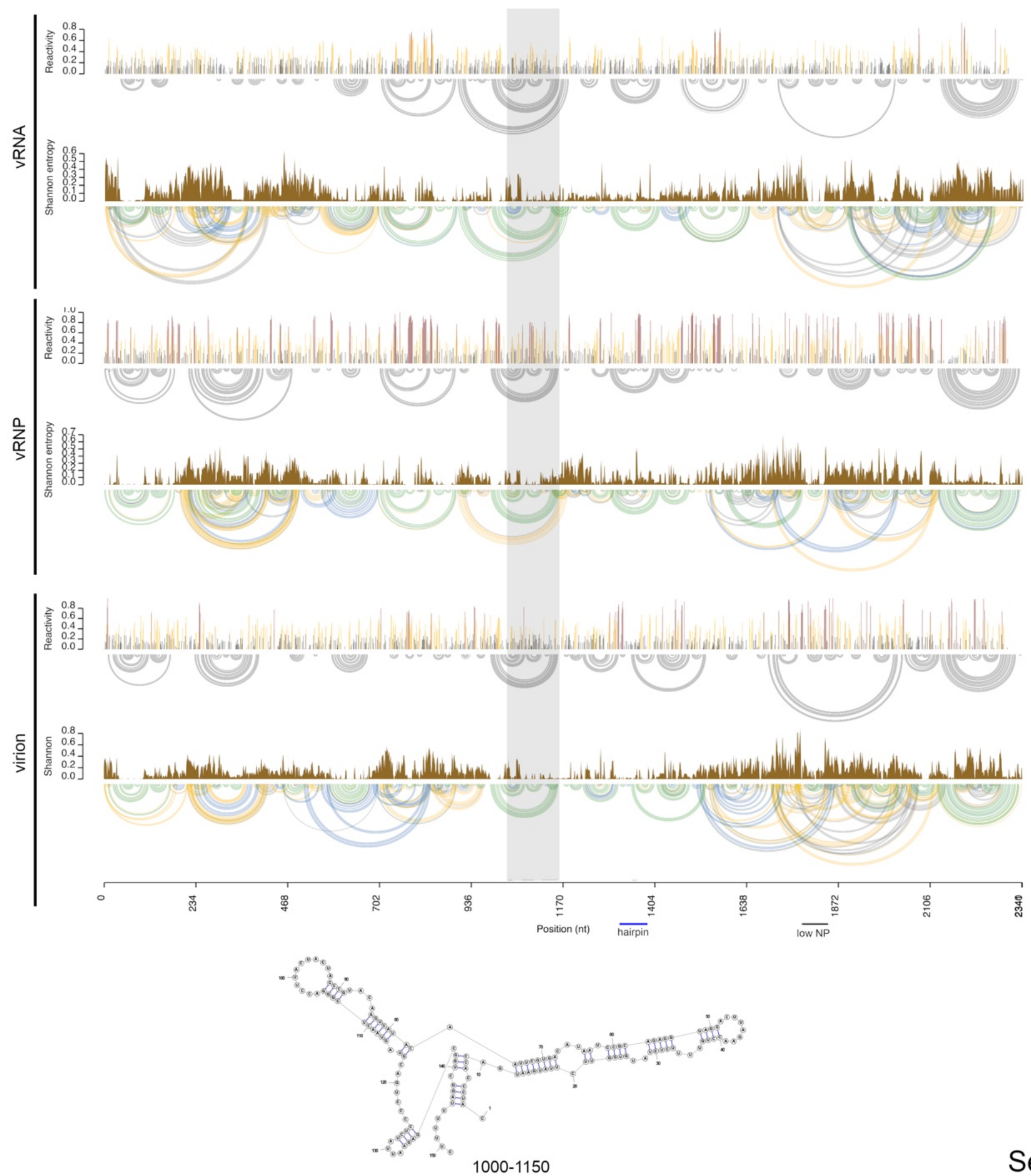


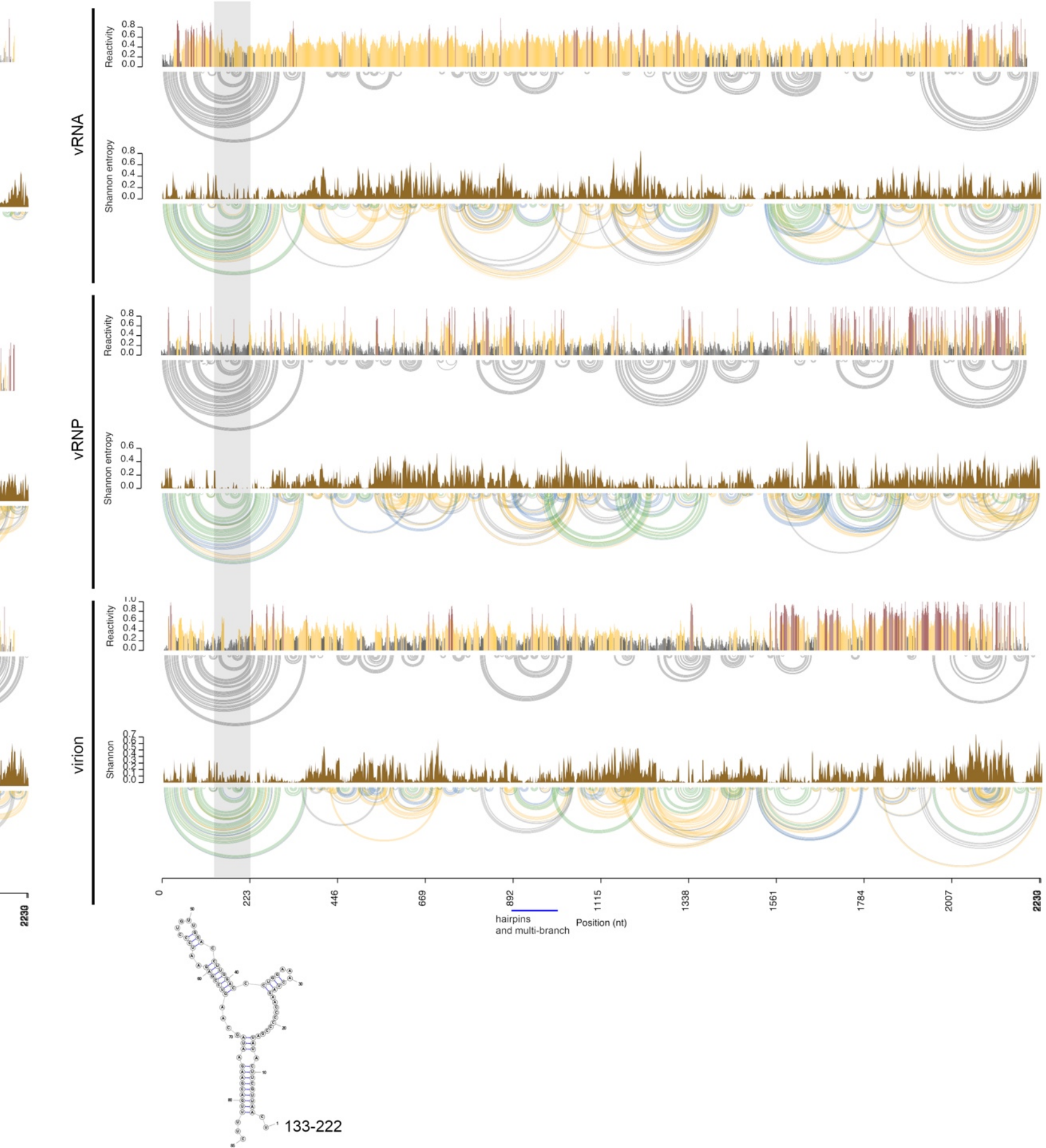
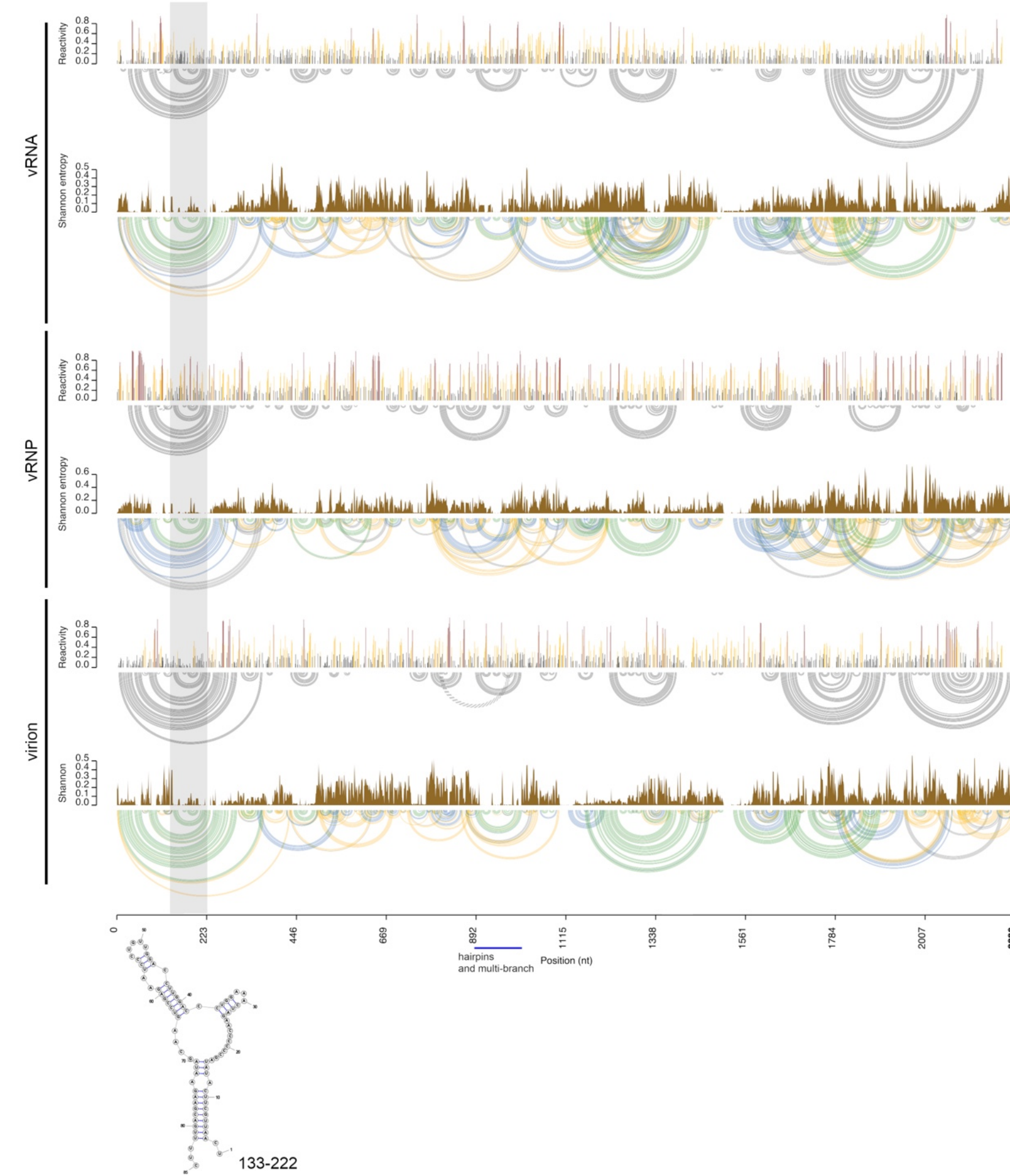
Figure S3



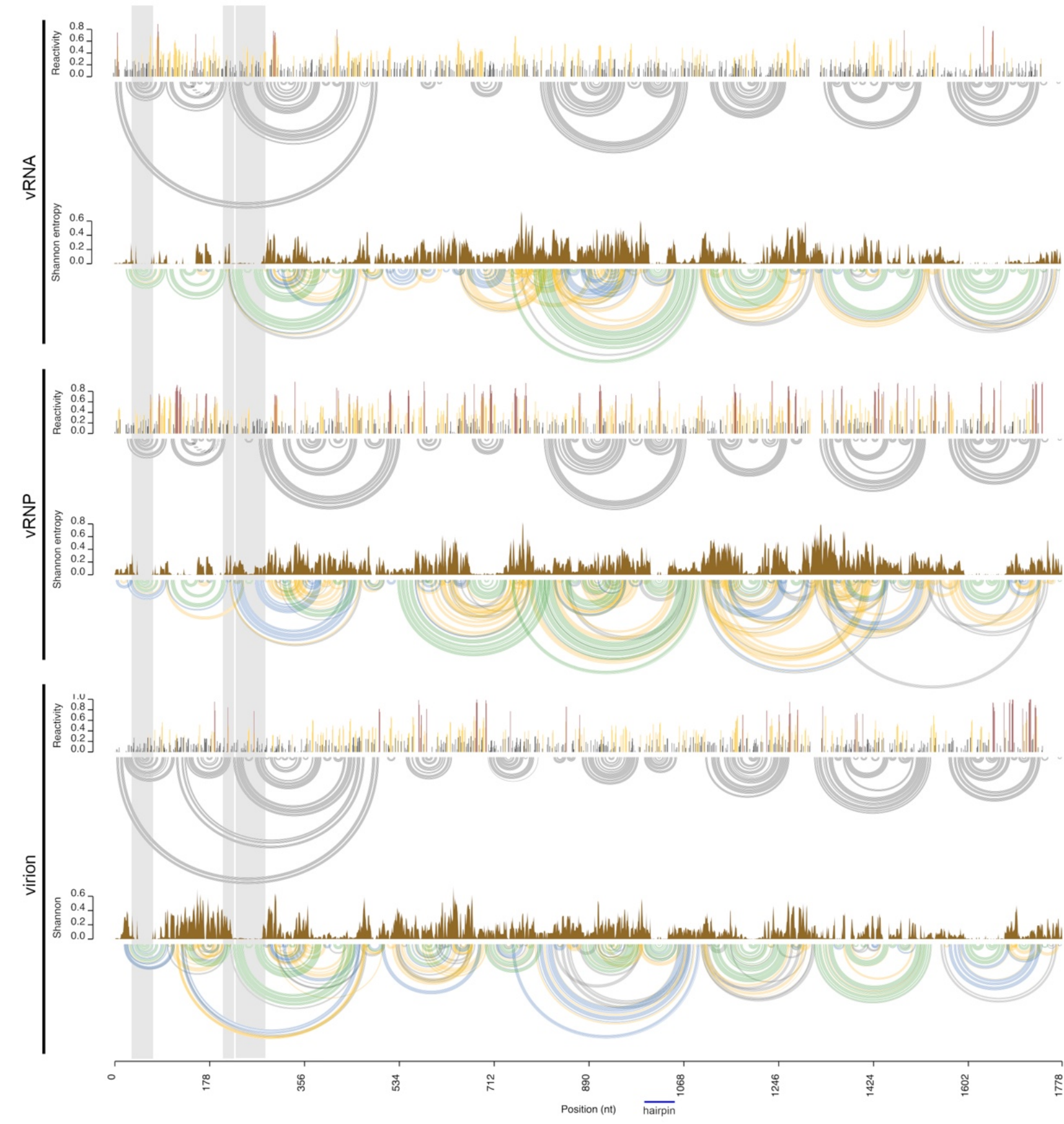
Segment 1



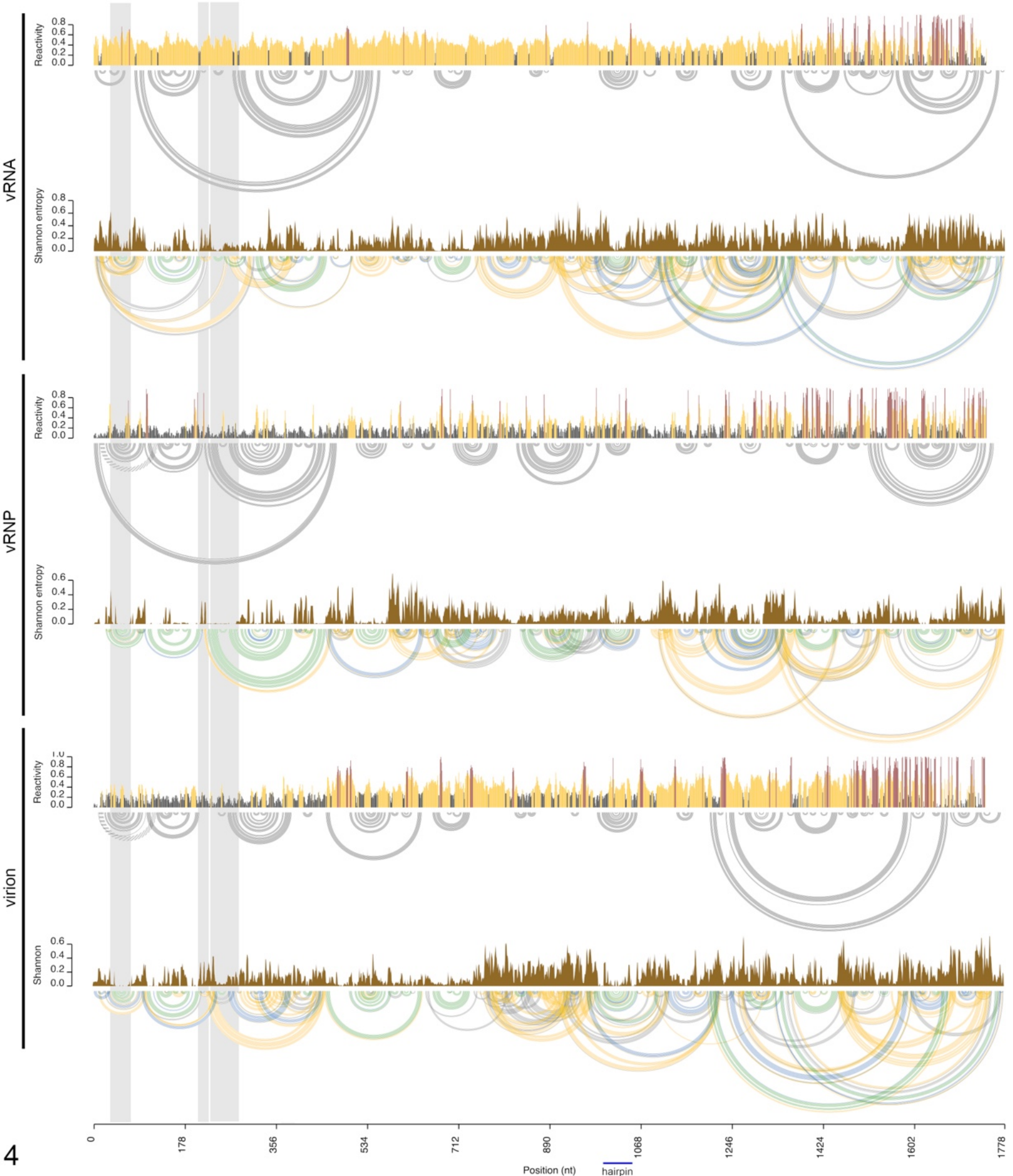
Segment 2

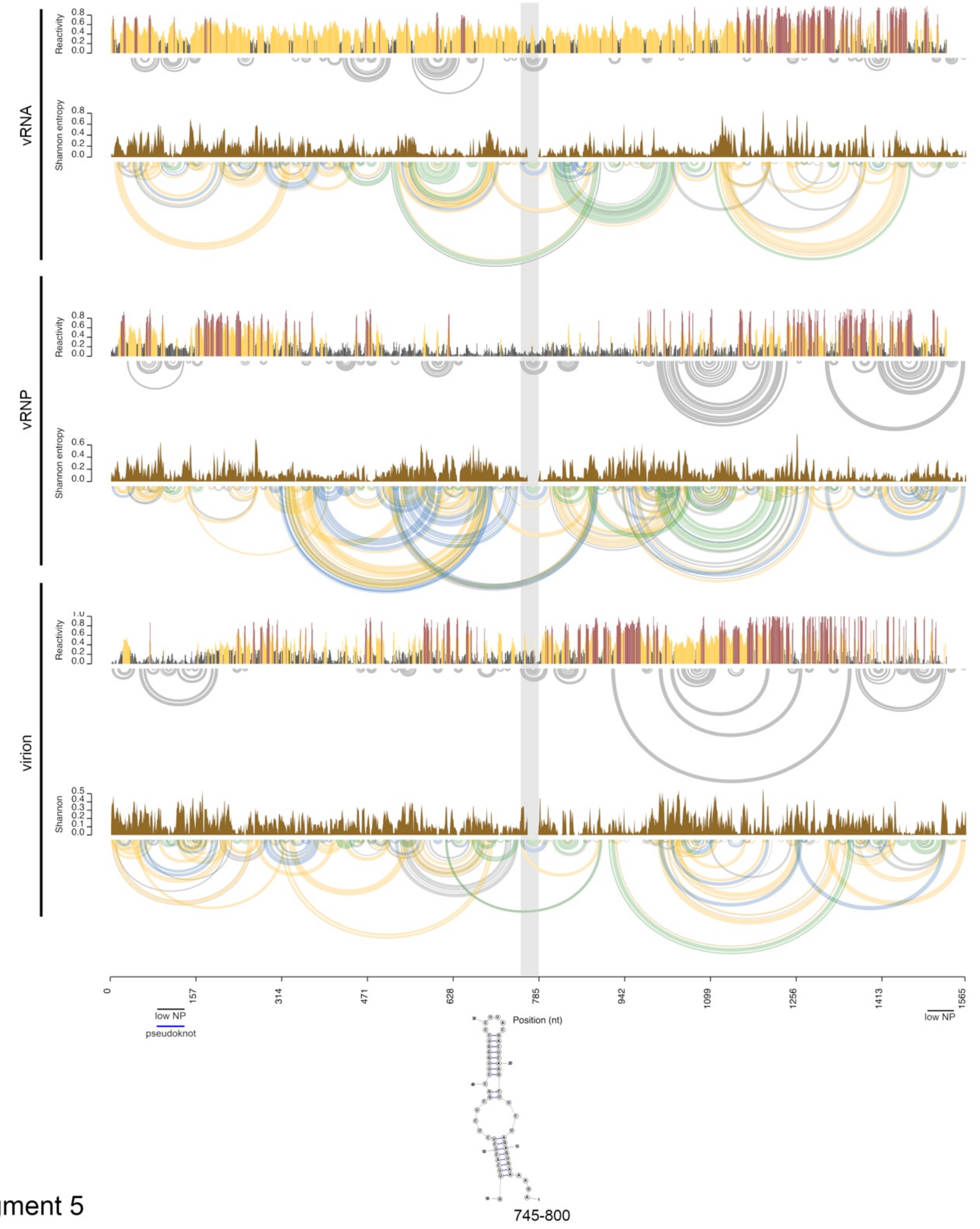
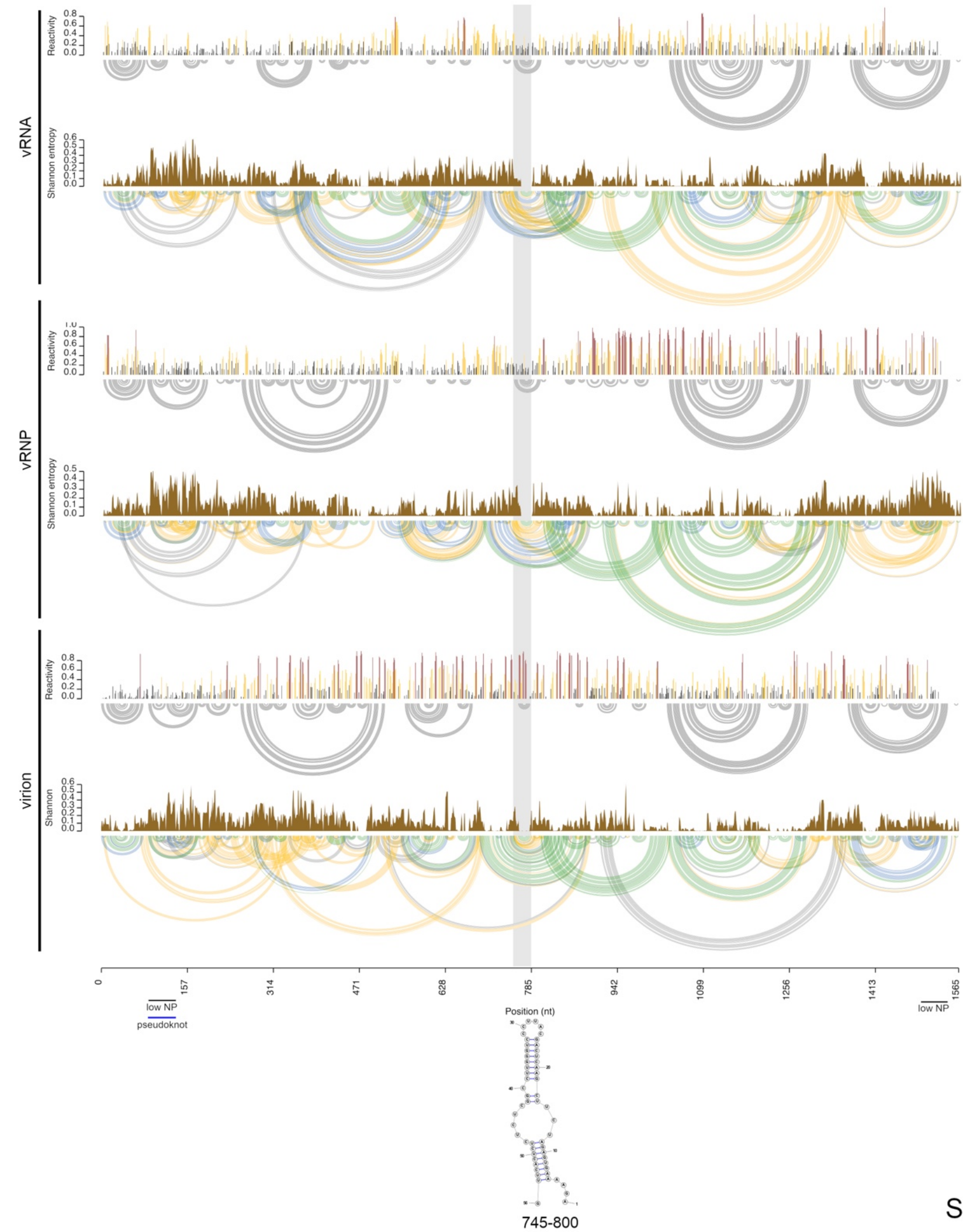


Segment 3

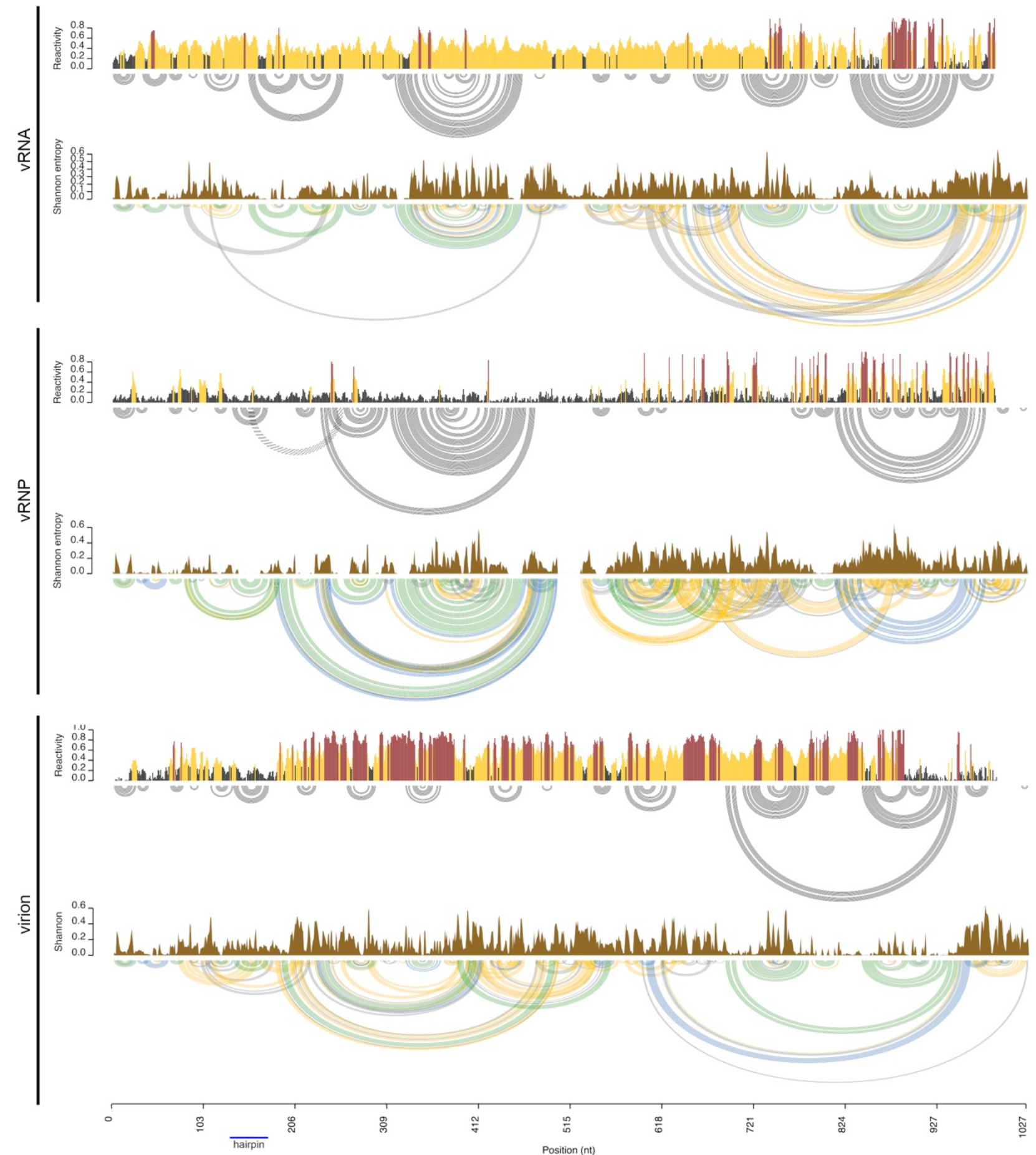
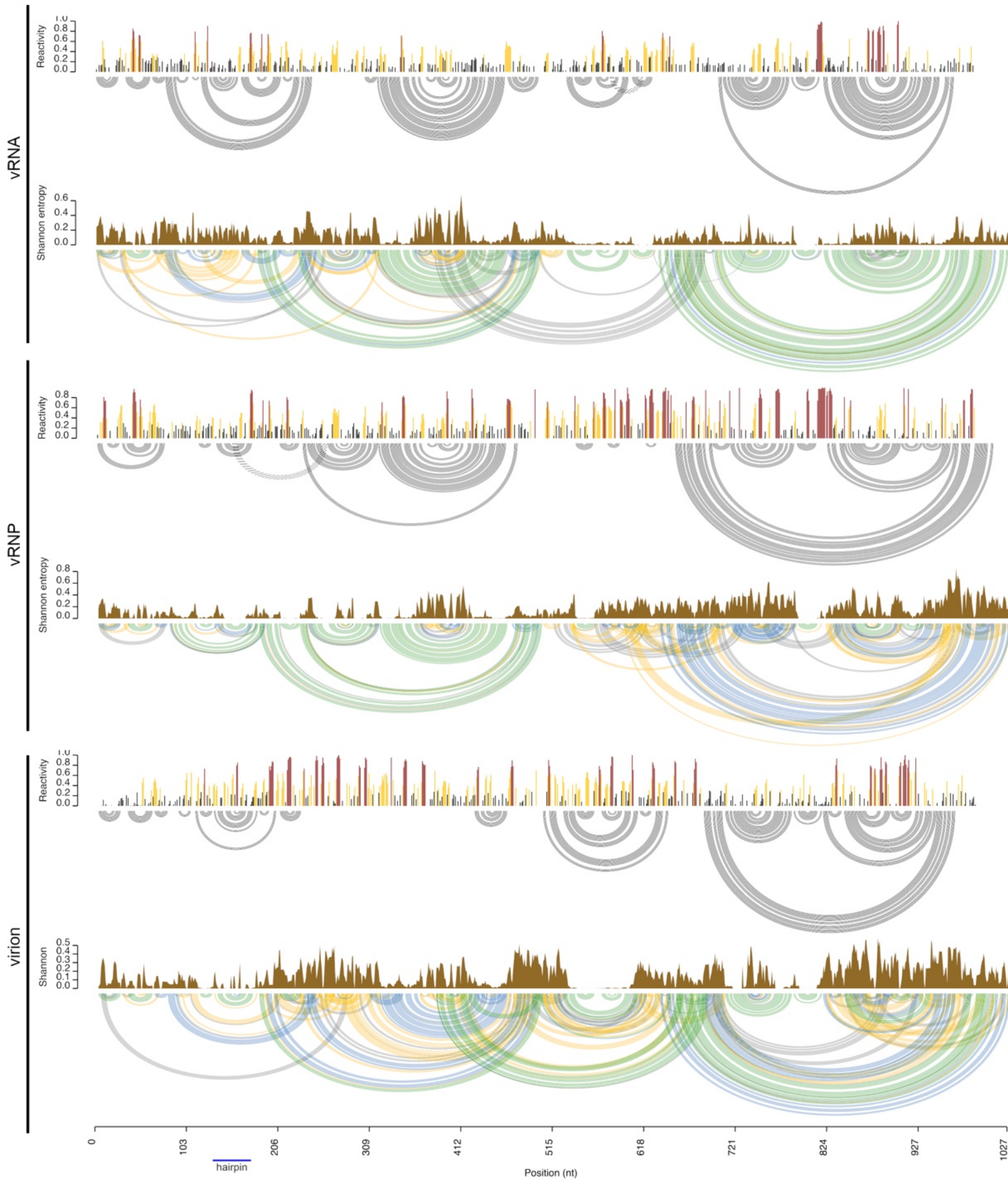


Segment 4





Segment 5



Segment 7

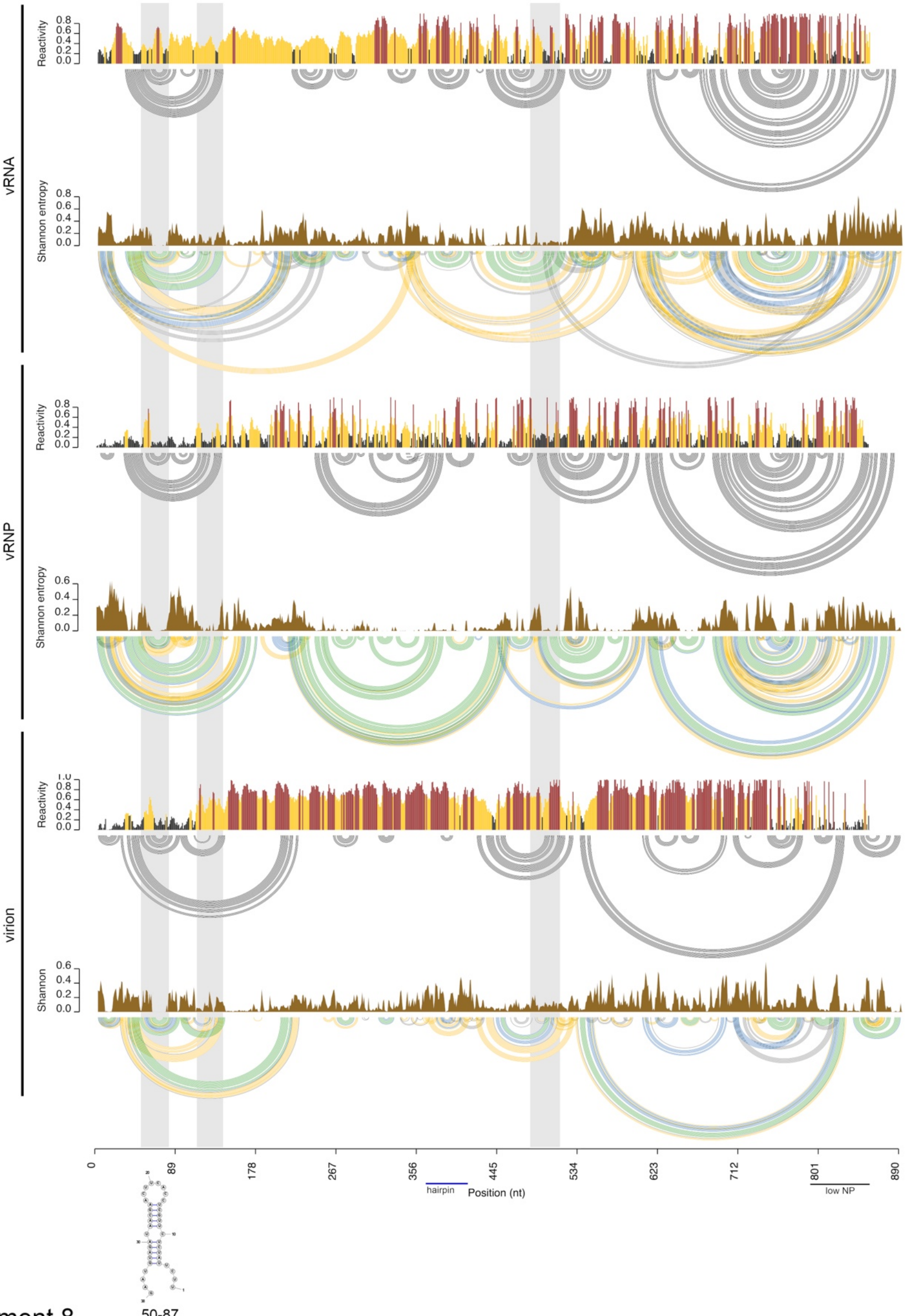
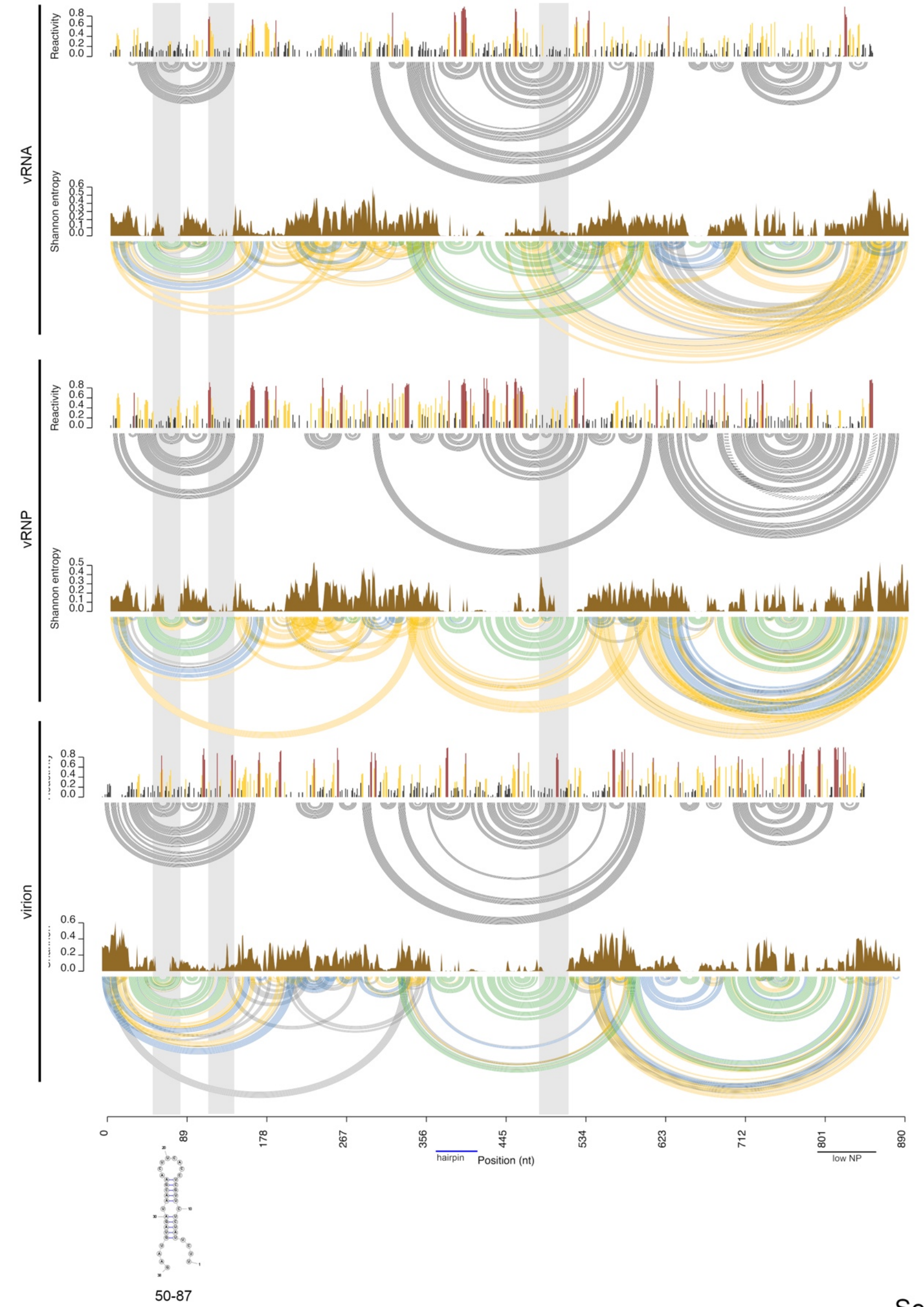
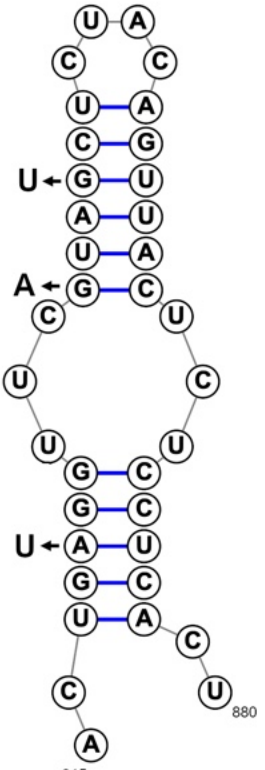


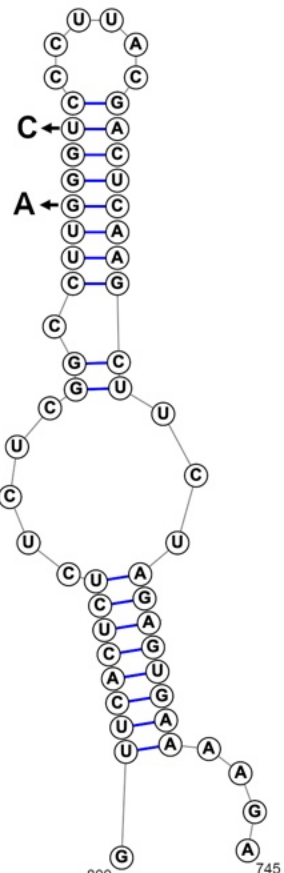
Figure S4



Seg1 880mut

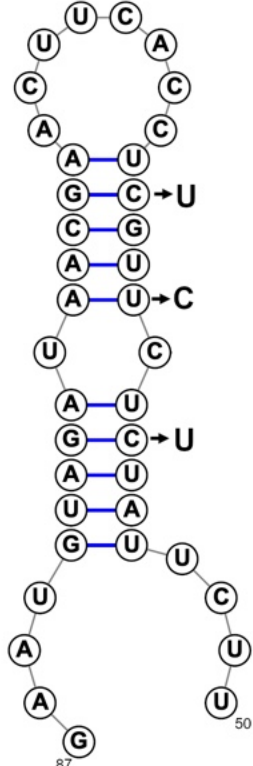
1.20

Median of CLIP/  
control reads:



Seg5 745mut

1.63

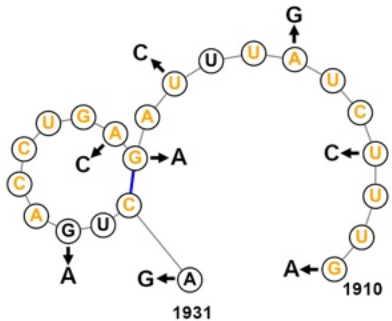


Seg8 50mut

1.04

Figure S5

A



Seg2 1910mut

Median of CLIP/control reads: 0.20

B

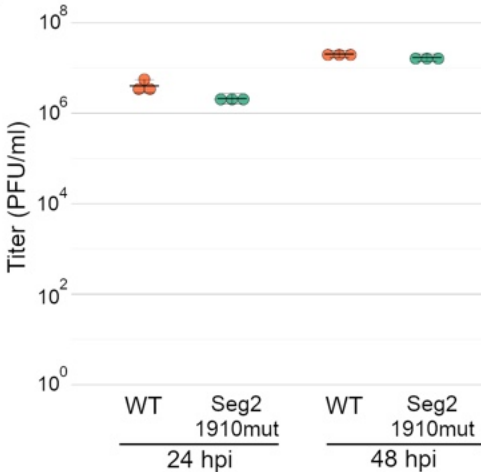
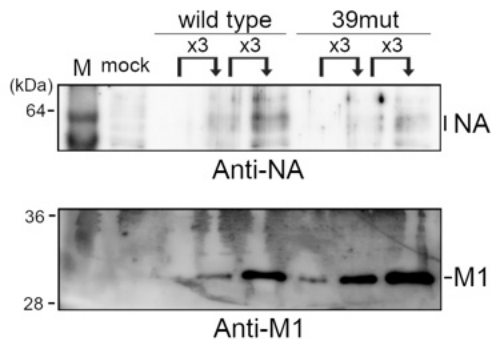
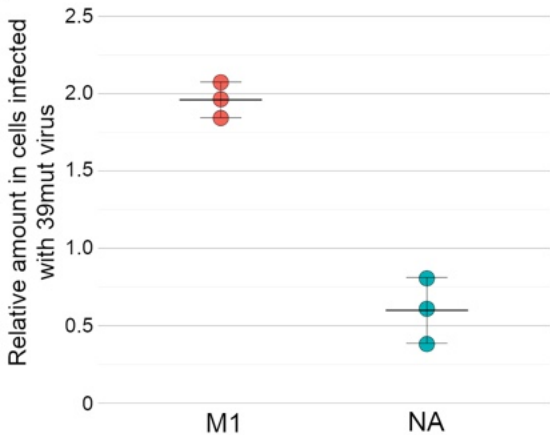


Figure S6

A



B



C

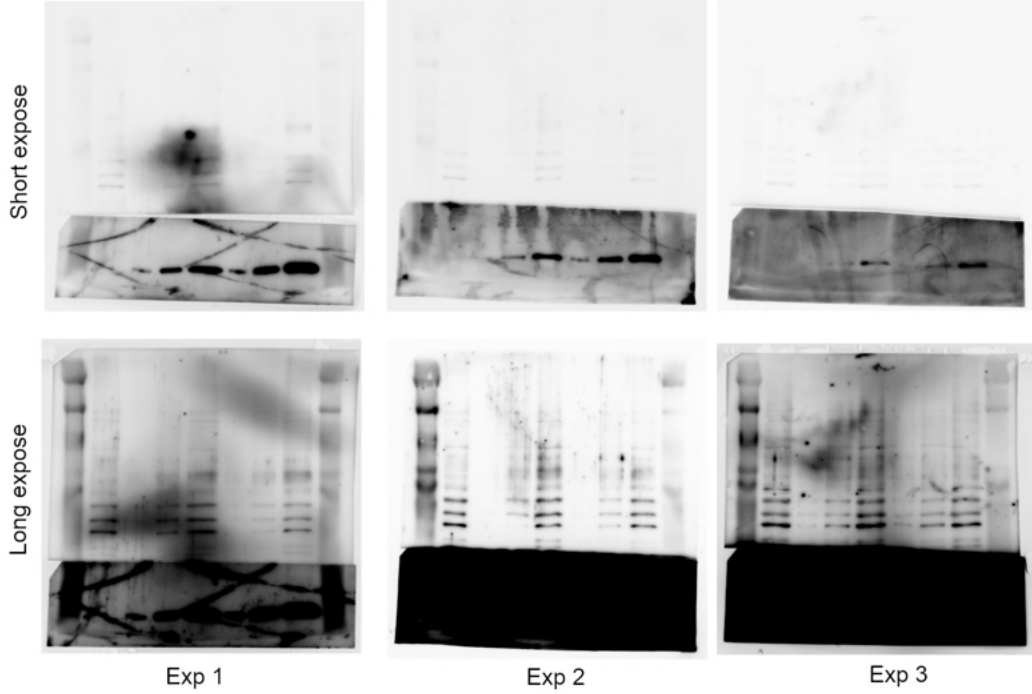


Figure S7

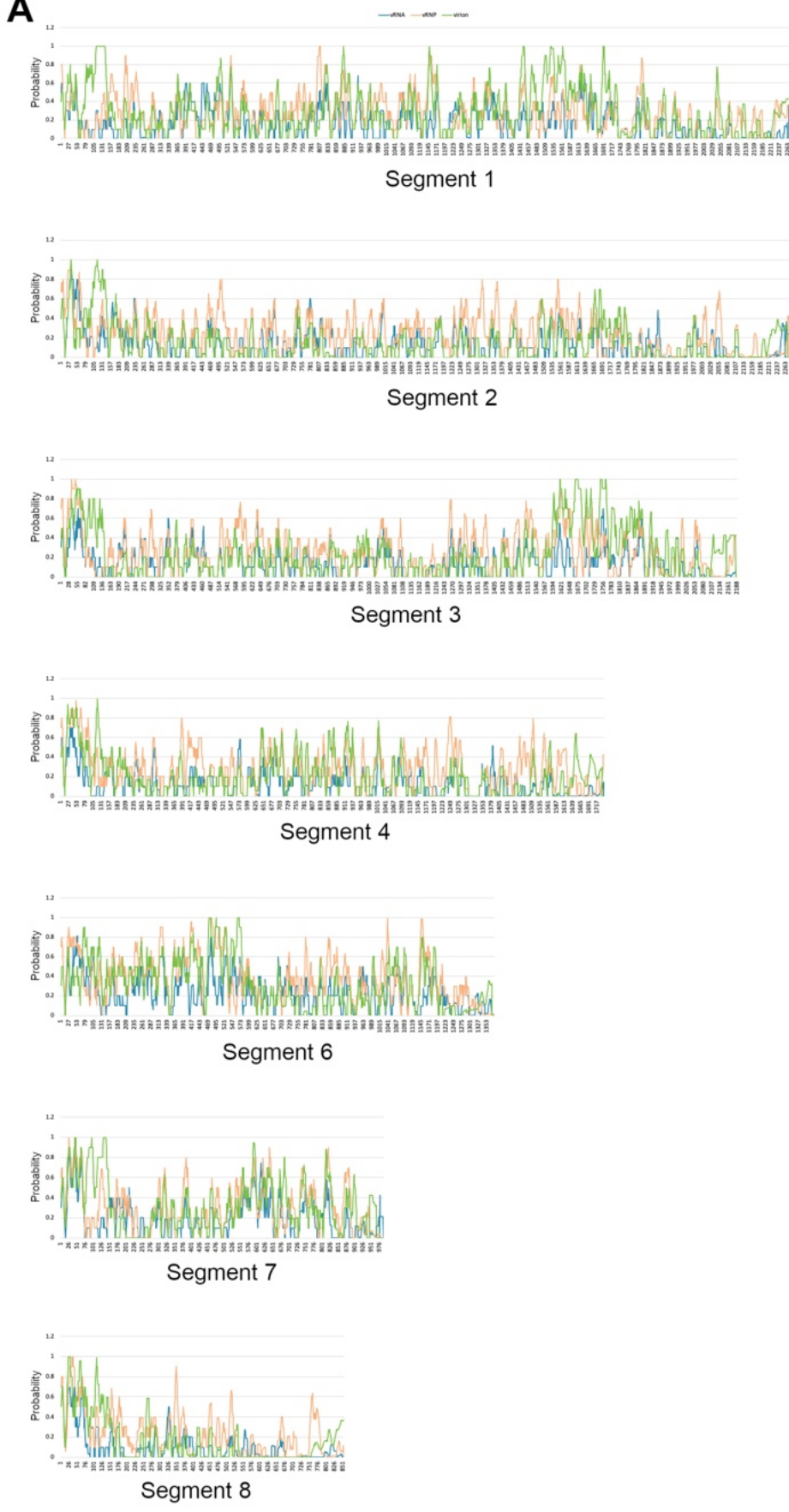
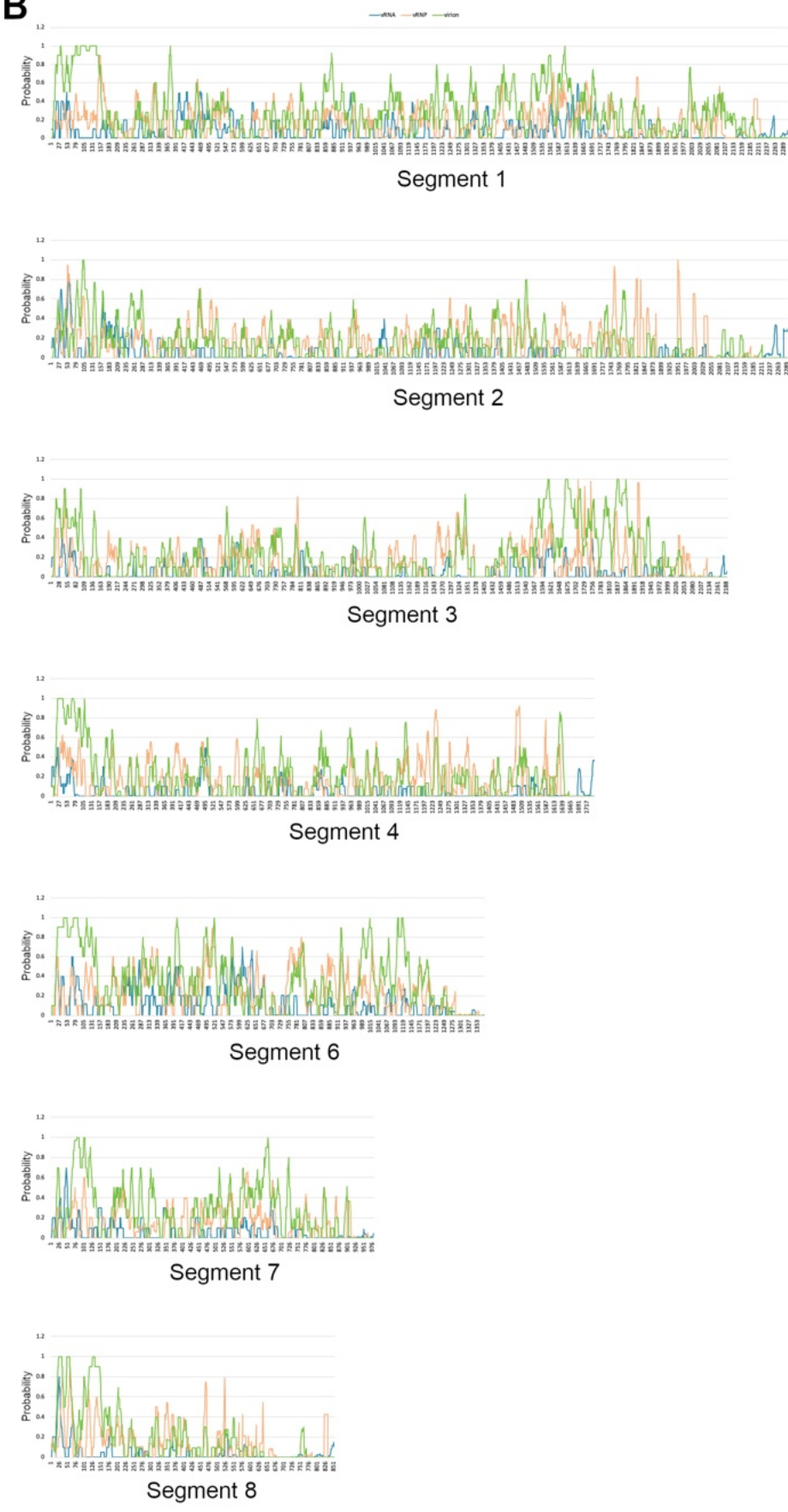
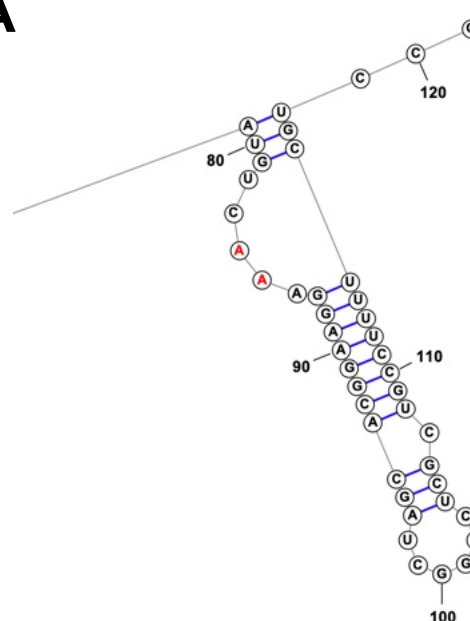
**A****B**

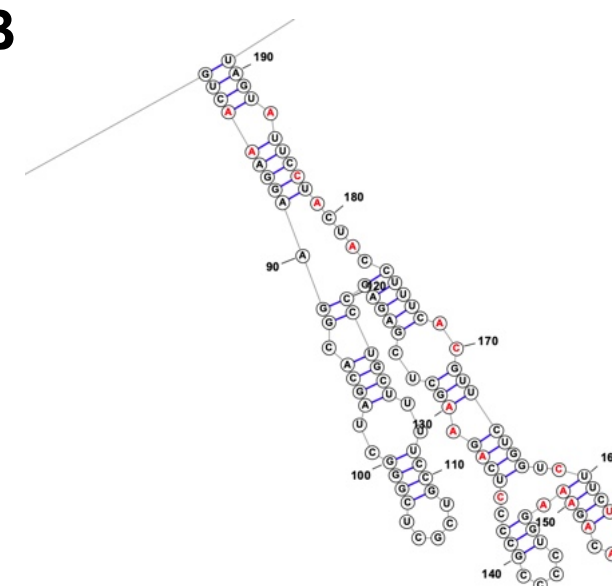
Figure S8

A



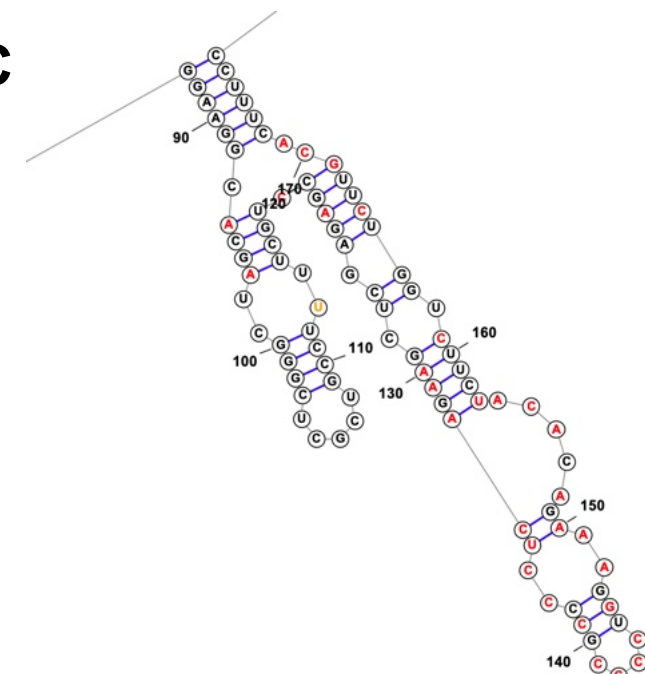
vRNA, DMS-seq  
5' stem-loop structure

B



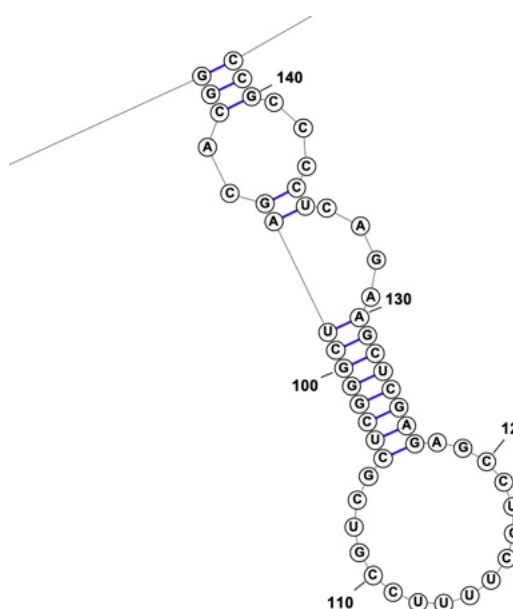
vRNP, DMS-seq  
multi-branch loop structure

C



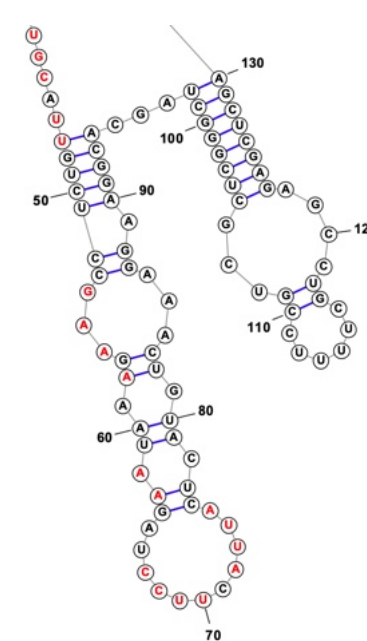
virion, DMS-seq  
multi-branch loop structure

D



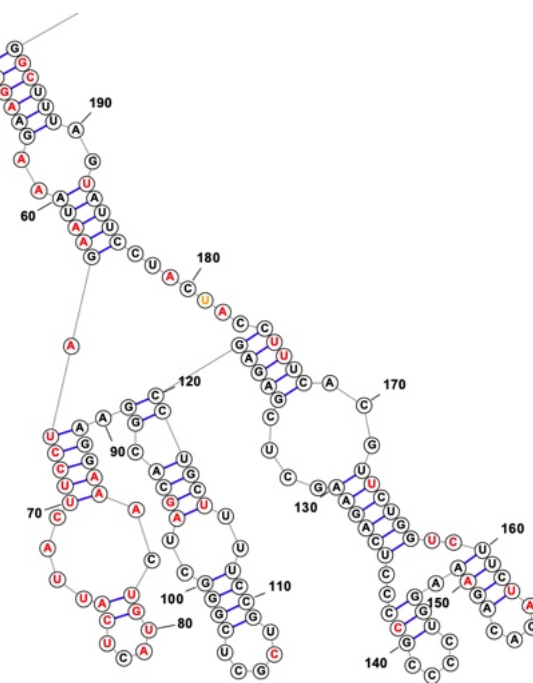
vRNA, SHAPE-seq  
3' stem-loop structure

E



vRNP, SHAPE-seq  
3' stem-loop structure

F



virion, SHAPE-seq  
multi-branch loop structure

# Figure S9

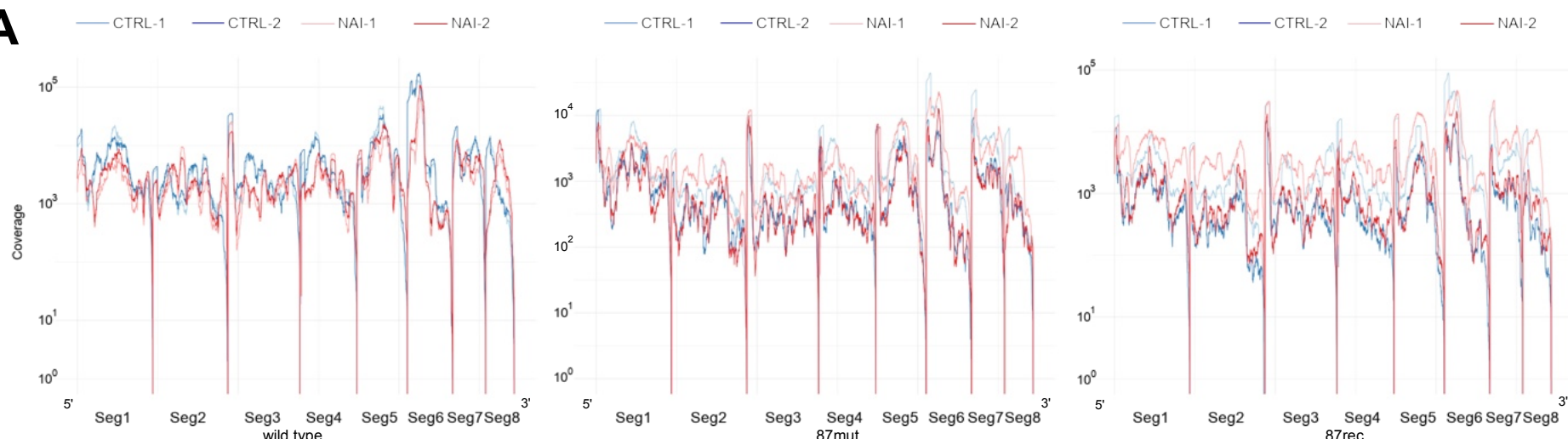
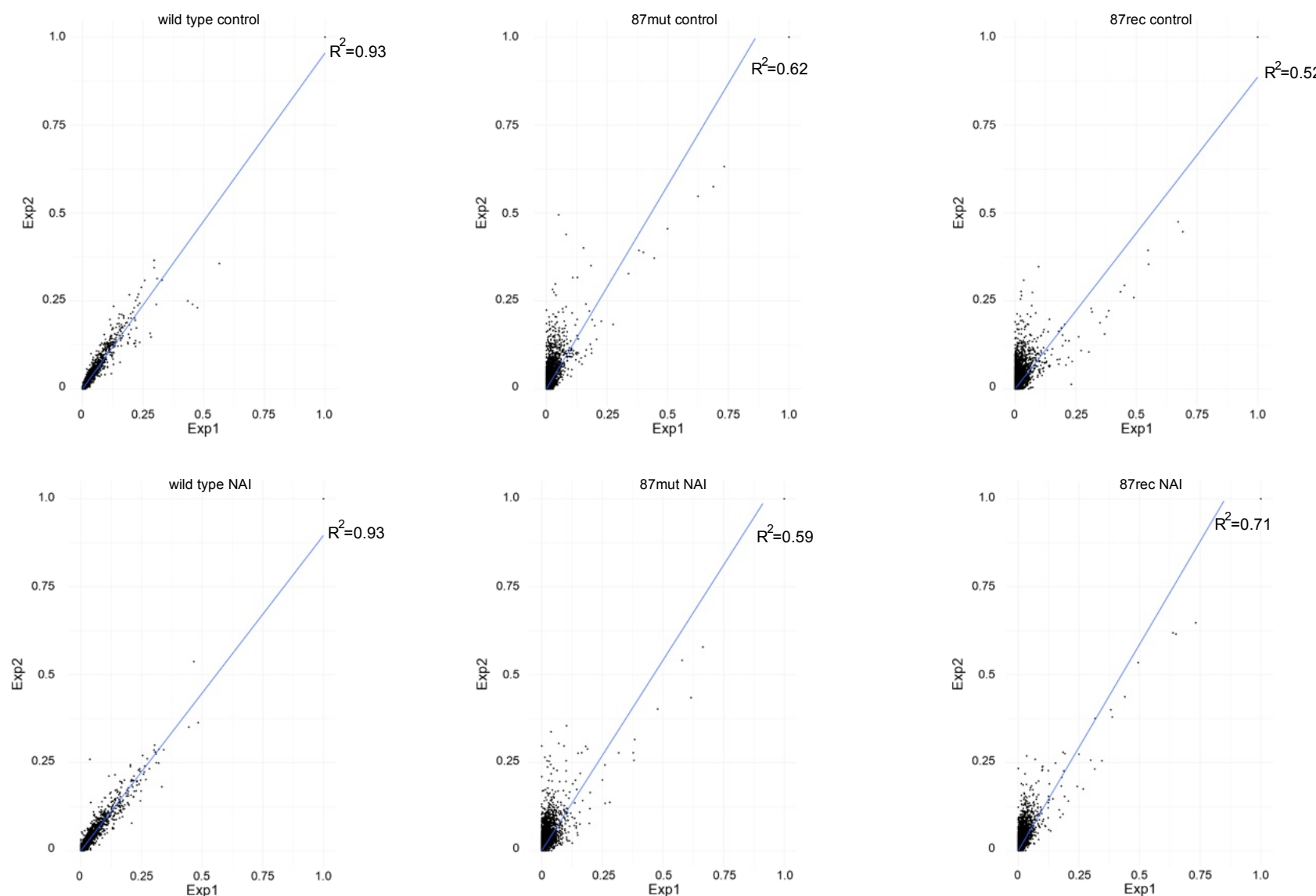
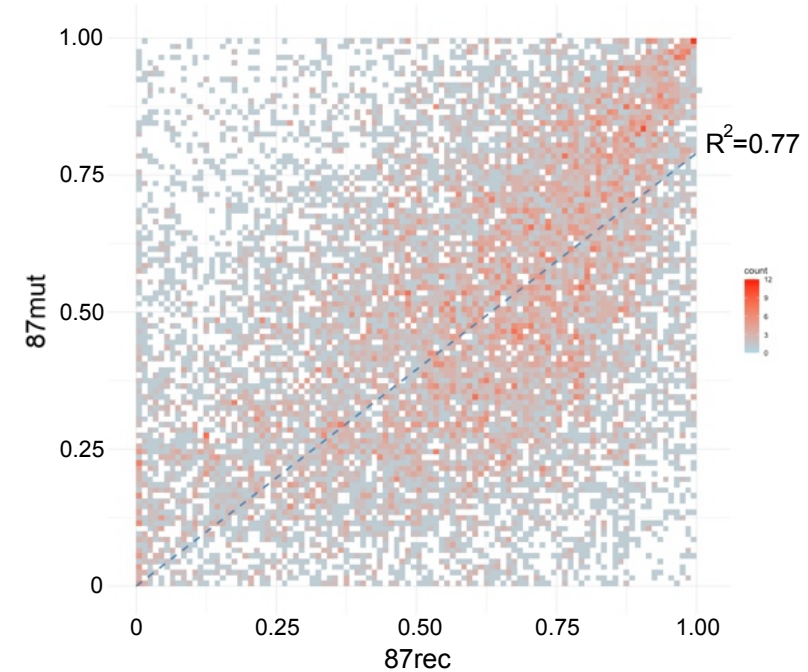
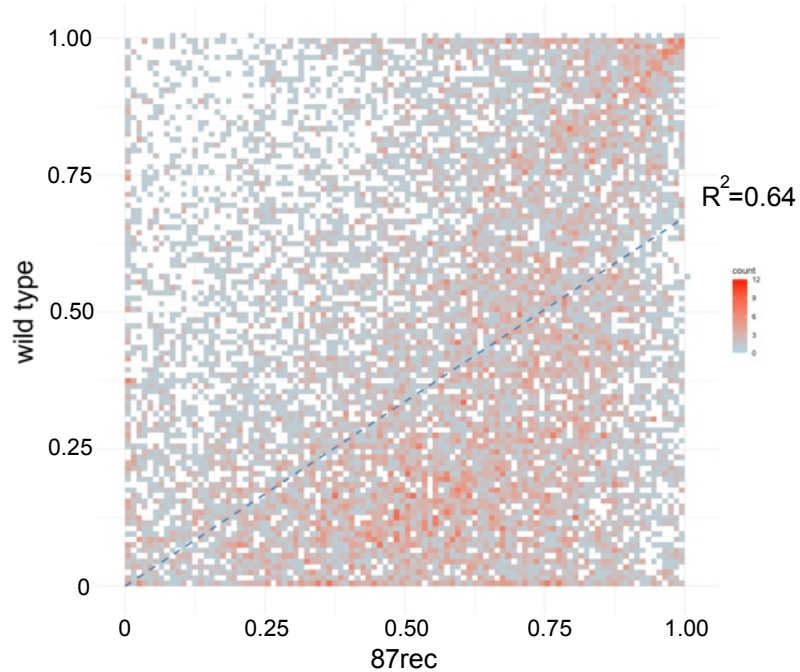
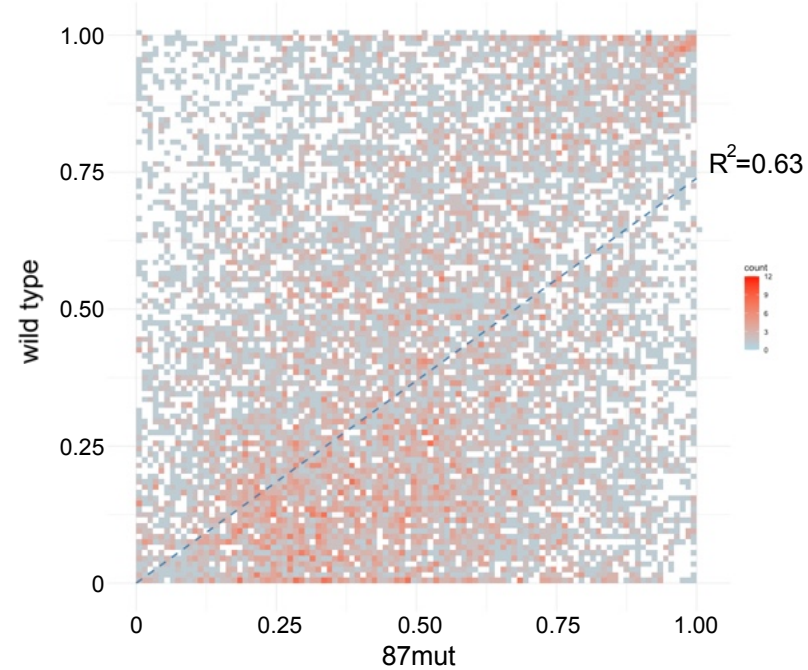
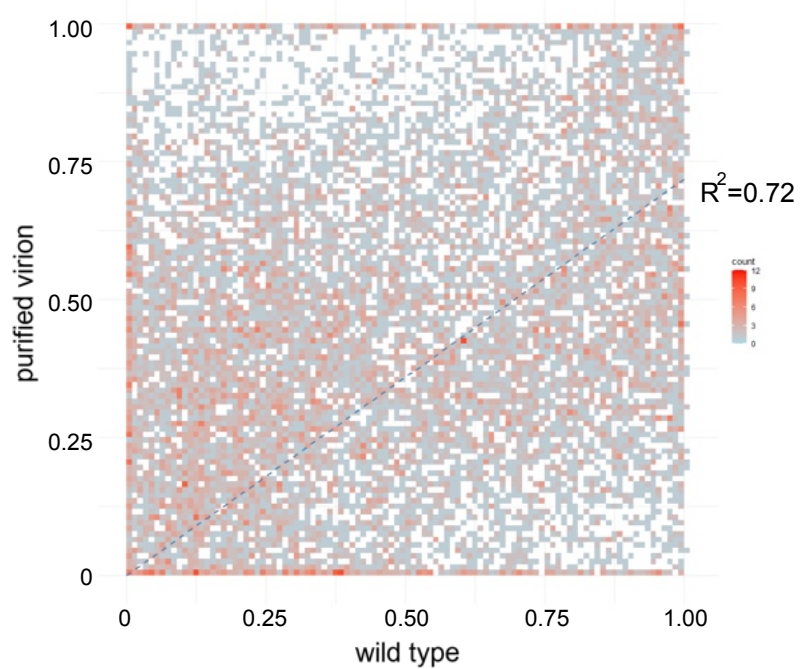
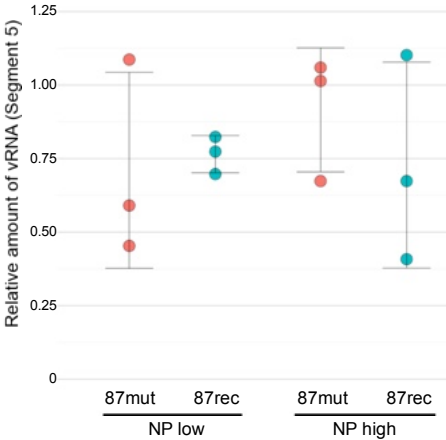
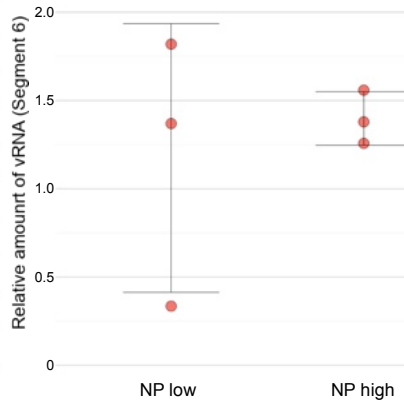
**A****B**

Figure S10



# Figure S11

**A****B**

**Figure S1. Coverage and drop-off rate of duplicate DMS-seq and SHAPE-seq. (A)**

Coverage of DMS-seq and SHAPE-seq. Coverages of mock-treated samples, DMS-treated samples, and NAI-treated samples were shown. (B) Scatter plot of drop-off rate from duplicate experiments. The drop-off rate is defined as the value of the stopped reverse transcription count divided by the coverage of each nucleotide, and the drop-off rates of duplicate experiments are plotted. The blue line means a regression line derived from the probabilities of modification of each nucleotide. The coefficient of determination ( $R^2$ ) is shown in each graph.

**Figure S2. Validation of DMS-seq and SHAPE-seq data. (A)** The base ratio of reverse

transcriptase drop-off site. Reverse transcriptase stop sites of duplicated control (CTRL-1, CTRL-2), DMS treated (DMS-1, DMS-2), and NAI treated samples (NAI-1, NAI-2) were counted, and the base ratio was calculated. (B and C) ROC curves and Precision-Recall (PR) curves of vRNA, vRNP, and virion samples. ROC curves and PR curves were drawn from the probability of modification from SHAPE-seq and DMS-seq and the structure model constructed from SHAPE-seq and DMS-seq. ROC-AUC was calculated and shown in the figure. The dot line area in the left panel of PR curves is enlarged in the right panel. (D) Correlation of Shannon entropy from SHAPE-seq and DMS-seq. The

Shannon entropy of each nucleotide position from SHAPE-seq and DMS-seq are plotted. Shannon entropy is divided into 100 bins from 0 to 1, and the number of counts in each bin is indicated by the colors shown in the figure. The blue line means a regression line derived from the probabilities of modification of each nucleotide. The coefficient of determination ( $R^2$ ) is shown in each graph. (E) Correlation between SHAPE-seq probability and SHAPE-MaP reactivity of the previous study. SHAPE-MaP reactivity of the previous study was divided into five groups, and the box plot indicates the distribution of SHAPE-seq probability in each group. P-values were calculated by Wilcoxon rank sum test and corrected by Bonferroni method.

**Figure S3. Base-pairing probability and Shannon entropy from DMS-seq and SHAPE-seq.** Base-pairing probabilities and Shannon entropies of each segment from DMS-seq (left) and SHAPE-seq (right) were calculated from the output of reactIDR by rf-fold. Base pairs were plotted as arcs, and green arcs, blue arcs, yellow arcs, and grey arcs in the Shannon entropy plot indicate a base-pairing probability of 80%, 30%, 10%, 3% or higher, respectively. Gray boxes indicate identified structured regions. Black lines indicate low-NP binding regions identified by PAR-CLIP (Williams GD et al., 2018). Blue lines indicate secondary structure regions identified by SHAPE-seq (Dadonaite B et

al., 2019).

**Figure S4. The schematic representation of mutation positions in Seg1 880mut, Seg5**

**745mut, Seg6 810mut, and Seg8 50mut recombinant viruses.** The secondary structure of the indicated region was predicted by RNAstructure. The predicted structures with maximum expected accuracy were shown, and mutations introduced in the recombinant viruses were indicated.

**Figure S5. The propagation of Seg2 1910mut recombinant virus. (A)** The schematic

representation of mutation positions in Seg2 1910mut recombinant virus. The SHAPE-annotated secondary structure of the indicated region was predicted by RNAstructure. The predicted structure with maximum expected accuracy was shown, and mutations introduced in the recombinant viruses were indicated. Red letters and yellow letters indicate probabilities of modification of more than 0.80 and 0.40, respectively. (B) Virus propagation of the Seg2 1910mut virus. MDCK cells were infected with the wild type or Seg2 1910mut virus at an MOI of 0.01. The supernatant was collected at indicated hours post-infection (hpi), and the virus titer was determined by a plaque assay. The crossbars indicate average values with standard deviations from three independent experiments.

The circles indicate the titer of each experiment.

**Figure S6. Expression of viral proteins in cells infected with Seg6 39mut**

**recombinant virus.** MDCK cells were infected with the wild type or Seg6 39mut virus.

The amount of M1 and NA at 8 hpi was determined by western blotting (A). The band intensity was quantified, and the relative amount of M1 and NA in cells infected with the Seg6 39mut virus was shown in (B). The crossbars indicate average values with standard deviations from three independent experiments. The circles indicate the titer of each experiment. (C) Raw images of western blot membranes. The membrane was cut, and the high molecular weight side was immersed in an anti-NA antibody and the low molecular weight side in an anti-M1 antibody. The upper panel shows short exposed membranes, and the lower panel shows long exposed membranes. The amount of M1 was quantified from short expose results, and the amount of NA was quantified from long expose results.

**Figure S7. Probabilities of modification from DMS-seq and SHAPE-seq calculated**

**by BUMHMM.** Moving average of probabilities of modification calculated by BUMHMM from DMS-seq (A) and SHAPE-seq (B). Y-axis: probability of modification. X-axis: nucleotide position.

**Figure S8. Predicted structures around nucleotide positions 87 – 130 of segment 5**

**from whole segment structure models.** RNA structures around nucleotide positions 87 – 130 of segment 5 predicted in Figure S4 are shown. (A-C) Predicted structures of vRNA (A), vRNP (B), and virion (C) from DMS-seq. (D-F) Predicted structures of vRNA (D), vRNP (E), and virion (F) from SHAPE-seq. The yellow and red letters indicate that the probabilities of modification by BUMHMM is greater than 0.4 and 0.8, respectively.

**Figure S9. Coverage and drop-off rate of duplicate SHAPE-seq of the wild type,**

**87mut, and 87rec viruses.** (A) Coverage of SHAPE-seq of the wild type, 87mut, and 87rec viruses. Coverages of mock-treated and NAI-treated samples of the wild type, 87mut, and 87rec viruses were shown. (B) Scatter plot of drop-off rate from duplicate experiments. The drop-off rates of duplicate experiments are plotted. The blue line means a regression line derived from the probabilities of modification of each nucleotide. The coefficient of determination ( $R^2$ ) is shown in each graph.

**Figure S10. Correlation analyses of probabilities of modification between the wild**

**type and mutant viruses.** The probability of modification of each nucleotide position

calculated from SHAPE-seq of the purified wild type virus from cell culture supernatant (wild type) and that from allantoic fluid (allantoic fluid) (upper left), wild type virus and 87mut virus (upper right), wild type virus and 87rec virus (lower left), and 87mut virus and 87rec virus (lower right) are plotted. The probability of modification is divided into 100 bins from 0 to 1, and the number of counts in each bin is indicated by the colors shown in the figure. The blue line means a regression line derived from the probabilities of modification of each nucleotide. The coefficient of determination ( $R^2$ ) is shown in each graph.

**Figure S11. Minireplicon assay using 87mut and 87rec of segment 5 and Seg6 39mut of segment 6.** Relative vRNA amount in cells transfected with the 87mut and 87rec vRNA templates (A) and the Seg6 39mut vRNA template (B). The amount of vRNA segment determined by RT-qPCR is normalized by that from the cells transfected with the wild type vRNA templates. The ratio of each polymerase subunit expression plasmid to NP expression plasmid is 1:1 in NP-high samples and 25:1 in NP-low samples.